Tellus (2006), 58A, 254–262
Printed in Singapore. All rights reserved

TELLUS

Diurnal circulation of the South American Altiplano: observations in a valley and at a pass

By JOACHIM REUDER[1] and JOSEPH EGGER[2*], [1]*Geophysical Institute, University of Bergen, Allégaten 70, 5007 Bergen, Norway;* [2]*Meteorologisches Institut, Universität München, 80333 München, Theresienstrasse 37, Germany*

(Manuscript receive 7 April 2005; in final form 30 September 2005)

ABSTRACT

In 2003, two quasipermanent stations have been installed at the Bolivian Altiplano in order to study the diurnal circulation of this huge meridionally oriented plateau at an altitude of ∼4000 m above msl. The station Tambo Quemado is located at the eastern side of a pass leading from the Altiplano down to the Pacific in the west. The station Rio de La Paz is positioned in a valley leading from the eastern lowlands to the city of La Paz. The data from these stations are analyzed mainly on the basis of master equations. The coefficients of a master equation are based on the observations and give the transfer rates of flow states in the phase space of selected observed variables like the horizontal wind components at a station. At Tambo Quemado, there is easterly upslope wind after sunrise but westerly inflow to the Altiplano takes over in the afternoon. Perturbations of this diurnal system with westerlies throughout the day are not uncommon. The diurnal flow system in the valley of the Rio de La Paz is extremely regular in that upvalley flow invariably becomes intense around noon. The nocturnal flow is weak without a preferred direction. It is a surprising result that the downvalley flow is moister than the upvalley flow. This finding and additional measurements downstream from the station suggest that at least part of the upvalley flow does not originate in the lowlands but descends from higher levels.

1. Introduction

The South American Altiplano is one of the grand plateaus on the earth with a fairly flat plain at an altitude of ∼4000 m bordered in the east and west by huge meridionally oriented cordilleras. As stressed by Flohn (1953), such a plateau acts as an elevated heat source during the day. The air above the Altiplano is warmer than above the lowlands in the east and west because of sensible heat transfer from the ground and partly also due to latent heat release above the plateau. In turn, one expects to find a diurnal circulation of the Altiplano with inflow during the day, where the passes leading to the Chilean deserts in the west and to the subtropical lowlands in the east provide the main gateways (see also Zängl and Egger, 2005, and references therein). Quite recently, in situ observations (Egger et al., 2005) showed indeed that this inflow at passes begins a few hours after sunrise to continue at least till sunset. The depth of the inflow layer is comparable to that of the convective boundary layer established above the Altiplano. There are indications of return flow above the inflow. The observations described in Egger et al. (2005) have been made in austral winter because fair weather at the Altiplano is normal at this time of the year. Profiles of wind, pressure, and temperature have been obtained at six passes with typical observation periods of 2 d per pass. These profiles have also been recorded in the valley of the Rio de La Paz, which ascends from the eastern lowlands to reach the height of the Altiplano near La Paz. Although the observations of Egger et al. (2005) suggest strongly that the Altiplano has a diurnal circulation on winter days as anticipated, an even fragmentary inflow climatology cannot be based on such scarce observations. Therefore, quasipermanent stations have been installed at two inflow points in order to partly overcome this limitation. The first one is located at the ascent from the Altiplano to the pass Tambo Quemado which leads to the Chilean desert in the west and to the Pacific (Fig. 1) the second one in the valley of the Rio de La Paz mentioned above. The pass height is roughly 500 m above the Altiplano proper. The observations at this pass have been disappointing (Egger et al., 2005) because inflow from the west has not been observed despite fair weather and weak ambient winds. More recent numerical simulations (Zängl and Egger, 2005) indicate that inflow should be expected at Tambo Quemado at least late in the afternoon. Torrez et al. (2005), present and discuss various aspects of the observations made at this station. They point out that

*Corresponding author.
e-mail: j.egger@lrz.uni-muenchen.de

DOI: 10.1111/j.1600-0870.2005.00168.x

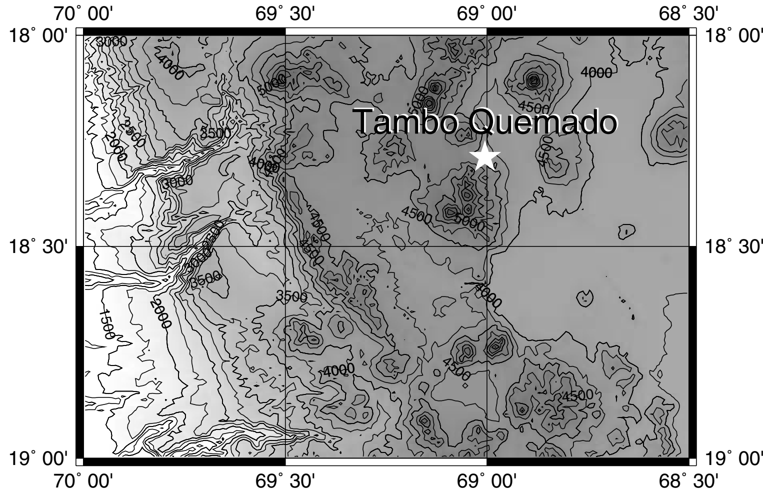

Fig 1. Terrain near the pass Tambo Quemado (contour interval 250 m). The star marks the location of the permanent station; shading is the darker the greater the altitude.

although the mean wind direction at Tambo Quemado is westerly, easterlies are common after sunrise. After noon, they become less frequent with increasing day time.

The valley of the Rio de La Paz is quite narrow and meandering strongly downstream of the permanent station. The simulations of Zängl and Egger (2005) capture the observations at this station quite well. They indicate, moreover, that there are powerful upvalley winds about 30–40 km downstream of the permanent station. The station Rio de La Paz is located about 200 km northeast of Tambo Quemado.

The permanent and autonomous stations contain instrumentation for temperature, relative humidity, pressure, wind speed, and direction. The instruments are mounted on a 3-m mast. Details on the instrumentation are given in Egger et al. (2002). It is the purpose of this article to present and discuss the data collected so far with particular emphasis on their relevance with respect to the diurnal circulation of the Altiplano. Master equations will be used as tools for the data interpretation. The derivation of these equations is outlined in the following section. The data collected at Tambo Quemado are presented and discussed in Section 3, those from Rio de La Paz in Section 4.

2. Master equation

Originally, master equations have been used in quantum mechanics (see Zwanzig, 2001, for a review) in order to describe the probabilistic behavior of quantum systems. While these equations were derived on the basis of theoretical arguments, it is also possible to construct master equations from data and to use them for an analysis of the observations and for probabilistic forecasts. Such equations have been used, for example, by Spekat et al. (1983) and Crommelin (2004) to study the variability of large-scale flow patterns. Here, we wish to learn more about the diurnal circulation of the Altiplano by discussing master equations based on the data collected at Tambo Quemado and Rio de La Paz. Master equations for valley flow data are presented in Egger (2002), where the emphasis is, however, on the relation of pressure differences between the two stations and related accelerations. Master equations for data from a single station have not been discussed as yet. Given the time series q_{1n}, q_{2n} of two variables q_1, q_2 at times $n\mathrm{D}t$ ($\mathrm{D}t = 5$ min; sampling interval), we span the phase space (q_1, q_2) of these two variables. This space is discretized by defining grid boxes (k,i) with

$$k\mathrm{D}q \le q_1 \le (k+1)\mathrm{D}q,$$

$$i\mathrm{D}q \le q_2 \le (i+1)\mathrm{D}q \tag{1}$$

and mesh size $\mathrm{D}q$. Any observed state (q_{1n}, q_{2n}) falls into one of these boxes. Notation is simplified by defining an index $s = K(i-1) + k$ (where K is the total number of grid boxes in q_1-direction) so that a box is characterized by just one number. In addition, we introduce here as a novel feature a gross discretization with respect to day time. Valley flows in the morning differ, of course, from those in the afternoon. It makes little sense to lump all these situations together. Instead, an index j is introduced to classify events according to day time. More specifically, an interval $\mathrm{D}\tau = 3$ h is used to define eight classes so that all events in the interval $0\ \mathrm{h} \le t \le 3$ h in the morning fall into the first class, etc. Related conceptual problems will be discussed below.

The mean probability $\hat{f}_s^j$ to find an event in the box s given the class j is estimated from the data by counting the number N_s^j of events where (q_{1n}, q_{2n}) is found in box s and in class j. The probability is normalized such that

$$\sum_s \hat{f}_s^j = 1. \tag{2}$$

The transition probabilities $T_{ss'}^j$ describe the probability that the system jumps from s to $s' \neq s$. An obvious estimate is

$$T_{ss'}^j = S_{ss'}^j / N_s^j \tag{3}$$

where $S^j{}_{ss'}$ is the observed number of jumps. The corresponding master equation

$$f_s^{jn+1} = -\sum_{s'} T_{ss'}^j, f_s^{jn} + \sum_{s'} T_{s's} f_{s'}^{jn} + f_s^{jn} \tag{4}$$

is essentially an equation of continuity which redistributes the probability densities according to the observations. In particular, f_s^{jn} is the probability to find the system in box s at time n.

The mesh size Dq is the same throughout the phase plane according to (1). This choice of discretization has the disadvantage that mean densities differ widely from box to box. Transition probabilities are difficult to determine for boxes which are rarely visited. This problem can be circumvented by choosing boxes of different size but equal mean density (e.g. Crommelin, 2004). There is, however, no unique rule how to construct these boxes. Moreover, visualization of transition fields becomes difficult in that case.

In steady-state, the sum of all transitions from one box (s) to all others must equal that from all other boxes to (s), that is,

$$\sum S_{ss'}^j = \sum S_{s's}^j. \tag{5}$$

In that case, we may insert the observed mean distribution $\hat{f}_s^j$ in (4) to find with (3)

$$\hat{f}_s^j = -\sum_{s'} S_{ss'}^j + \sum_{s'} S_{s's}^j + \hat{f}_s^j \tag{6}$$

so that $\hat{f}_s^j$ is a steady solution to (4) because of (5). If, however, the flow in class j is not statistically stationary, (5) is not satisfied. If, for example, q_1, q_2 are the horizontal wind components and if there is a general increase of upvalley flow speeds in the class $j = 4$ (9–12 h), the boxes with high speeds contain more cases at the end of this interval than at the beginning. This implies a mean transfer of states during this interval so that (5) is not satisfied. That leads to an unrealistic convergence of states if (4) is integrated for such a class for times much longer than Dτ.

The subdivision of all events into classes with respect to time introduces the additional problem that states occupied in one class may not be occupied in the following one. Thus an integration of (4) may lead to the situation that a switch from index j to $j + 1$ will leave states occupied which are not linked to other states in the class $j + 1$. Hence these populations have to stay unaltered till a class is initialized where those states are again part of the set. That occurs for certain after 1 d.

It is, of course, impossible to display all transfer coefficients. Instead, a mean transfer vector $(\mathbf{t}_1, \mathbf{t}_2)_{ki}$ per grid box is defined by summing over all transfer coefficients in one direction (see also Egger, 2001), so that

$$t_{1ki}^j = \sum_{k'>k} T_{ss'}^j - \sum_{k'<k} T_{ss'}^j \tag{7}$$

where the first (second) sum runs over all boxes with $k' > k$ ($k' < k$). A corresponding rate can be defined with respect to q_2 so that typical transfers are captured by the transfer vector $\mathbf{t} = (t_1, t_2)$. The maximum value, $|\mathbf{t}| = 1$ occurs, when all states leave the box within one time step in a certain direction. This transfer "velocity" describes the mean motion in the phase plane. If a forecast must be made for a state $(q_1^n,\ q_2^n)$, the transfer vector gives the most likely direction of change. Note that the components of the transfer vector do not have a dimension. The master equation represents, however, also the flow's random perturbations. Their impact is essentially diffusive and is not described by the transfer vector. A measure of the related spread d at a grid box $s \sim (k, j)$ is

$$\left(d_s^j\right)^2 = \sum_{s'} T_{ss'}^j [(k' - k)^2 + (i' - i)^2] \tag{8}$$

where $s' \sim (k', j')$. The spread d_s^j measures the extent of a cloud of states normalized by Dq after one time step which is first concentrated at box s with indices (k,i). For example, the spread is 1.2 if all states are transferred with equal probability $T_{ss'} = 0.125$ to the eight adjacent boxes. The spread is nondimensional.

The master equation (4) provides a statistical model for the data. A much simpler strategy is to use a regression model

$$q_k^{n+1^*} = \sum_m A_{km} q_m^{n^*} \tag{9}$$

($k, m = 1, 2$) where $q_k^{n^*}$ is a deviation from the time mean $\hat{q}_k$ and where the coefficients A_{km} follow from a least square fit of (9) to the observations. Unlike the coefficients of (4), those of (5) do not depend on the location of the state $(q_1^n,\ q_2^n)$ in the phase plane. In principle, a probability density can be predicted on the basis of (5), but the basic dynamics of (5) are so simple that this effort is not warranted. Solutions to (5) can be written down in terms of the eigenfrequencies λ_I and the corresponding eigenvectors. Contraction and eventual rotation are the only motions admitted by (5). Obviously, the master equation (4) provides a more detailed description of the system. Nevertheless, it is not clear a priori if the extra effort to analyze the master equation provides additional insight.

Note that, the transfer vector

$$(\mathbf{t}_1, \mathbf{t}_2) \sim (((A_{11} - 1)q_{1s} + A_{12}q_{2s}), (A_{21}q_{1s} + (A_{22} - 1)q_{2s})) \tag{10}$$

of the regression model (9) is simply proportional to the tendency. This transfer field is contracting because the eigenvalues of (9) have negative real parts. There is no diffusion in a regression model.

3. Tambo Quemado Pass

The terrain near the pass is displayed in Fig. 1. The pass is located at an altitude of 4600 m in between two volcanoes. The topography to the west of the pass is fairly complicated. In general there is descent to the Chilean desert but there is a further massif of ~4500 m height in the west. Any diurnal inflow from the west has to cross this barrier before it reaches Tambo Quemado. The fairly flat Bolivian Altiplano extends eastward

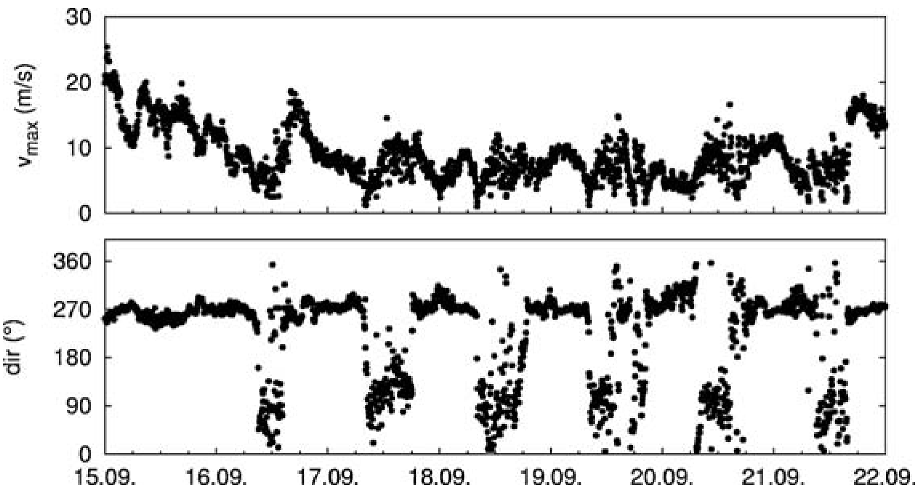

Fig 2. Time series of maximum wind speed per 5 min interval and direction for 15–21 September 2003 at Tambo Quemado (LST).

from the border station. Although it would have been best to install the station at the pass, the chances for destruction appeared to be too large. Instead, the permanent station is located near the Bolivian border station about 5 km to the east and a few 100 m below the pass proper. There, westerlies mean either inflow from Chile or downslope flow. Easterlies indicate upslope flow toward the pass.

Data have been collected continuously from August 19, 2003 to February 14, 2004. Technical problems prevented further data collection. All data presented here are averages over 5 min intervals (Dt = 5 min). Figure 2 shows wind speeds and directions for a week in September 2003. In general, winds are westerly but there is a period of mainly easterly winds around noon almost every day. The wind speeds are quite variable but there is a tendency for the velocities to peak after the period of easterlies came to an end. Velocities of more than 10 ms^{-1} are quite common.

Figure 3 shows the frequency distribution of observed wind speeds for all months where observations are available. Clearly, flow speeds tend to be lowest in austral summer while high speeds are common in winter and spring. Of course, Fig. 3 reflects not only seasonal changes of the diurnal circulation but also those of the large-scale circulation. Nevertheless, direct inspection of the time series shows clearly that weak winds tend to occur for easterly flow directions, that is, for upslope flow toward the pass.

We choose first the zonal wind component $u = q_1$ and the meridional one $v = q_2$ as variables in the master equation. They are normalized by their respective *SD* 5.8 (1.9) ms^{-1}. The daily mean wind ($\bar{u} = 5.4$, $\bar{v} = 0.5$ ms^{-1}) is westerly. The westerlies are strongest with $(\hat{u}, \hat{v}) = (8.7, 2.3)$ for $j = 6$ (15–18 h; ˆ

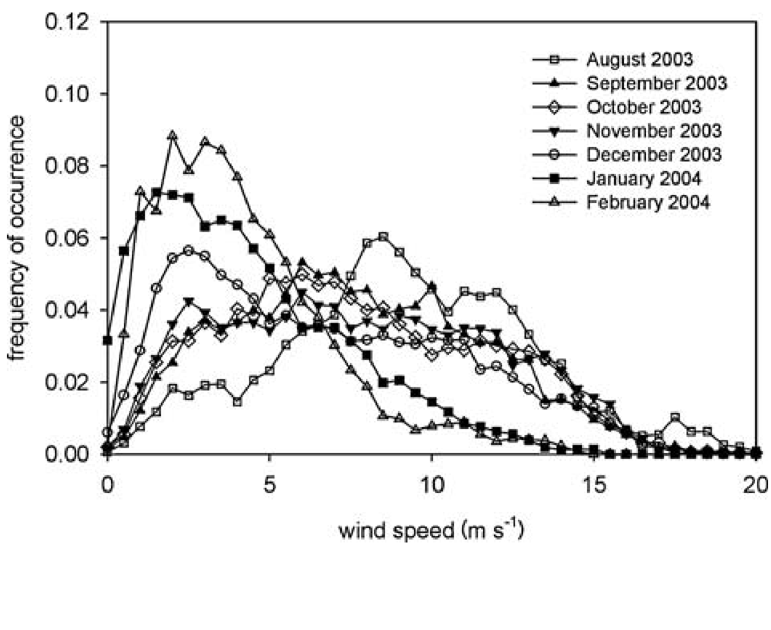

Fig 3. Frequency distribution of wind speed in (ms^{-1}) at Tambo Quemado for the months August 2003–February 2004.

interval mean). Easterlies prevail with (−0.4, 1.9) in the interval $j = 4$ before noon. In other words, the situation in Fig. 2 is typical. Distinct upslope winds ($u < -3$ ms^{-1}) are found on 136 out of 180 d. If there are intense upslope winds they tend to blow for about 2 h. There is no day without intense ($u >$ 3 ms^{-1}) westerlies at Tambo Quemado. Of course, the threshold of 3 ms^{-1} is somewhat arbitrary.

The eigenvalues of (9) are found to be negative for all the eight classes of a day. Typical damping times $(\lambda_I + 1)^{-1}$ are ∼1 h in the night but are reduced to ∼25 min during daytime. This reduction reflects the enhanced turbulence during the day. The absence of complex eigenvalues implies that all states move along straight lines toward the mean. To learn more about these flows we have to turn to the master equation (4).

The transfer vectors **t** for $j = 1$ and $j = 2$ (not shown) are contracting, the spread is ∼1−2 for the chosen mesh size Dq = 0.25 which corresponds with a velocity interval of 1.4 (0.5) ms^{-1} in $u(v)$-direction. The situation becomes interesting in the morning interval (6–9 h; $j = 3$) where two maxima of the density distribution are found (Fig. 4). A value of f ∼ 0.03 as found at the easterly maximum implies a probability of 3% to observe winds in the mesh box there. Clearly, the prominent maximum in Fig. 4 is due to the upslope winds developing after sunrise. The westerly less populated center represents those days when upslope winds develop late or when nocturnal westerlies continue throughout the day. The transfer vectors **t** (Fig. 5) for this situation converge toward the two maxima of the distribution in Fig. 4. The attraction of the upslope maximum is clearly larger than that of the westerly center. The maximum transfer velocity of 0.9 attained in this case

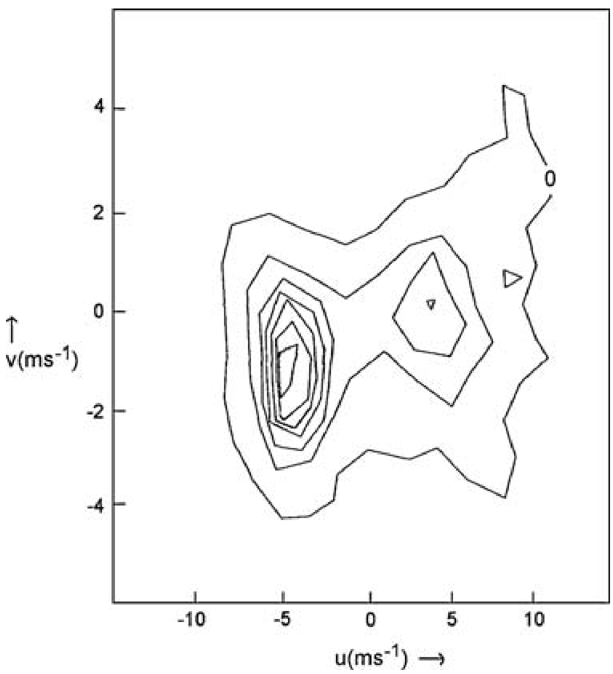

Fig 4. Density distribution f in the time interval (6–9 h; $j = 3$) in units 10^{-3} at Tambo Quemado for $q_1 = u$(ms^{-1}), $q_2 = v$(ms^{-1}). Contour interval 5. Note that the scaling is different for abscissa and ordinate, respectively, which reflects the different scaling for u and v; Dq = 0.25; bin size (1.4 ms^{-1} × 0.5 ms^{-1}).

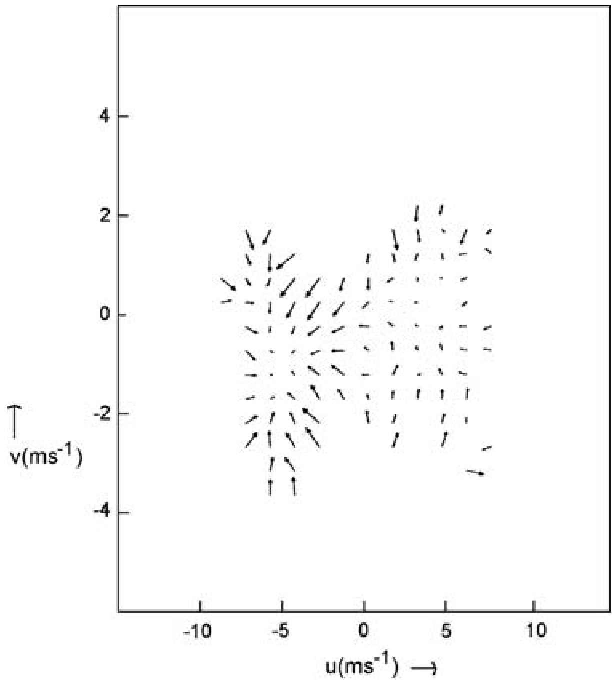

Fig 5. Transfer vector **t** in the interval (6–9 h) at Tambo Quemado for $q_1 = u$, $q_2 = v$. Maximum vector length 0.9. Gridboxes with less than 10 visits excluded; Dq = 0.25.

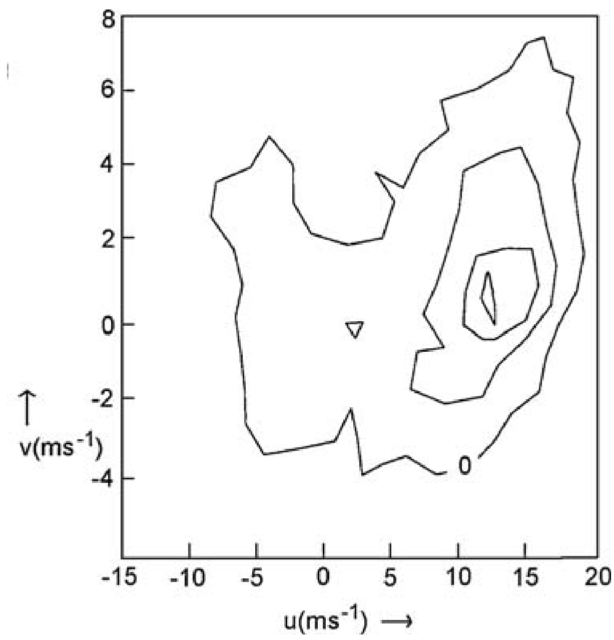

Fig 6. Density distributions f in the time interval (15–18 h; $j = 6$) in units 10^{-3} at Tambo Quemado for $q_1 = u$(ms^{-1}), $q_2 = v$(ms^{-1}). Contour interval 5.

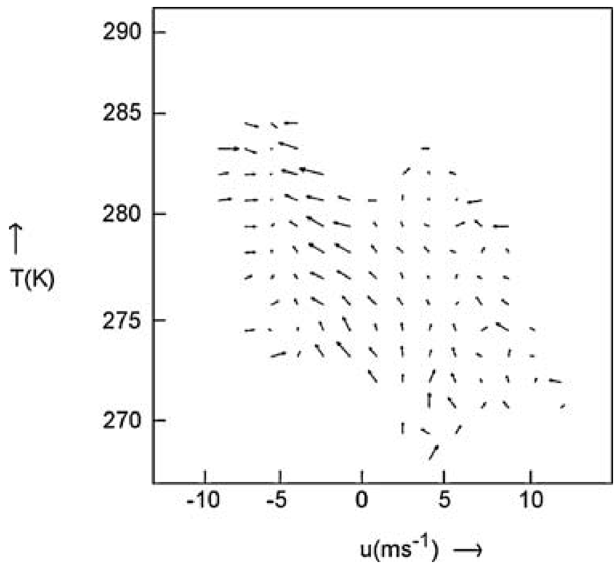

Fig 7. Transfer vectors **t** in the interval (6–9 h) at Tambo Quemado for $q_1 = u(\mathrm{ms}^{-1})$, $q_2 = T$ (K). Maximum vector length 0.82.

indicates that nearly all states leave the corresponding box during one time step. The regression model (9) is, of course, incapable of reproducing the transition vectors in Fig. 5.

Three hours later ($j = 4$; 9–12 h) the situation is essentially the same except that the winds are more variable. Moreover, a larger part of the phase space than in Fig. 4 is covered by the states. Typical values of the spread are 2–3 with somewhat larger values in the slope wind regime where spreads ∼4 are found. In that case, wind speeds change within one time step of Dt = 5 min by about one *SD*. In other words, the flows are highly variable. The easterlies begin to fade after noon and the westerly maximum is more densely populated in that interval. Hence, the diurnal circulation of the Altiplano with its inflow from the west is now taking over and suppresses the easterly slope winds. Later in the afternoon, the easterlies disappear almost completely (Fig. 6). There is now a well defined maximum of strong westerlies while the upslope regime contains few states. The transfer velocities are mainly contracting toward this maximum (not shown). The inflow toward the Altiplano weakens after sunset so that the center of the distribution is close to the climatological mean in the interval 18–21 h with spreads less than 2.

We are free with respect to the choice of variables for the master equation. The combination $q_1 = u$, $q_2 = T$ (temperature) is of particular interest in thermally driven flows. The mean temperature is 279 K with a *SD* of 5 K. The diurnal cycle spans almost exactly one *SD*. As before, the situation becomes interesting in the interval (6–9 h), where a clear upward tendency of the temperature is seen in Fig. 7 as is the tendency of the upslope winds to intensify and of the westerlies to weaken. The upslope easterlies are warmer than the downslope westerlies. This makes good sense for thermally driven slope winds. This difference of temperatures is seen even in the afternoon where easterlies tend to be slightly warmer than the westerlies. As we have seen, the easterlies do hardly exist in the interval before sunset when the temperature of the westerlies is beginning to fall.

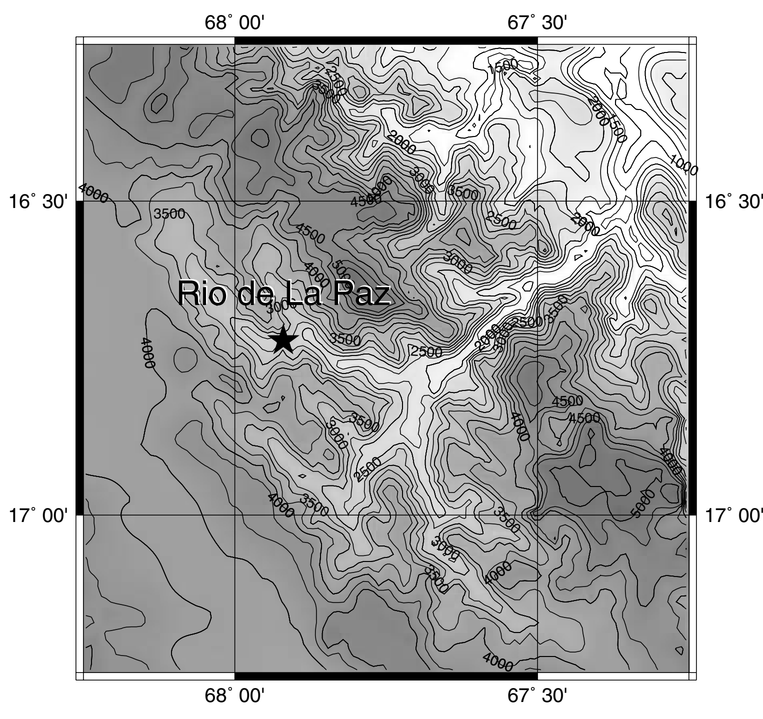

Fig 8. Terrain near the permanent station is the valley of Rio de La Paz. Contour interval 250 m; star: location of station; shading the darker the larger the altitude.

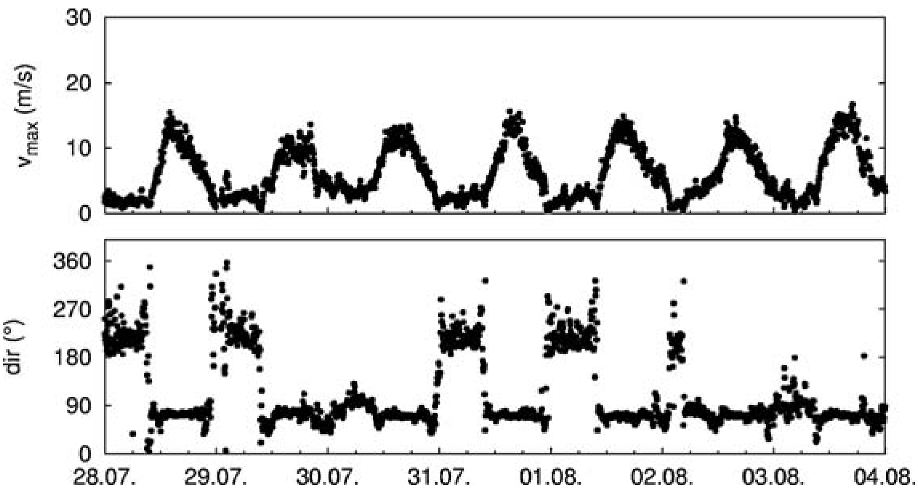

Fig 9. Time series of maximum wind speed per 5 min interval and direction at Rio de La Paz for the week 28.7.2003 to 4.8.2003.

The combination $q_1 = u$, $q_2 = \rho_v$ with water vapor density ρ_v gave fairly clear results. Easterlies tend to be moister than westerlies. The latter involve descent from the pass and are, therefore, less humid than the upslope winds originating at the Altiplano.

4. Rio de La Paz

The river descends from the Altiplano's altitude of $\sim$4000 m above msl down to the eastern lowlands at an altitude of $\sim$1000 m above msl (see Fig. 8). The main valley has three branches. The valley is oriented almost zonally near the permanent station which is located in the northwestern branch. A typical weekly time series of wind speed and direction is presented in Fig. 9. There is a rather regular and abrupt switch from the nocturnal downvalley wind regime with its small westerly velocities to the diurnal upvalley regime with easterly winds of 8–10 ms^{-1}. The corresponding monthly frequency distribution of wind speeds (Fig. 10) for July 2003 shows two peaks, a relatively sharp one for the nocturnal situation and a broad one for the upvalley flow regime. This distribution implies a great variability of the upvalley flow strength. Examples of this variability are provided in Egger et al. (2005) where strong winds were observed on July 19 and weaker ones on July 20, 2003. There is a tendency toward the merging of both peaks in austral summer. In February 2004, there is only one peak near $|v| \sim 3$ ms^{-1} and higher velocities occur rarely. Although it may seem to be counterintuitive that valley winds are weaker in summer where the insolation is strongest, we have to keep in mind that valleys winds are adjustment flows which are the less pronounced the weaker the stratification. Moreover, the intercomparison of the global radiation distribution for July 2003 and February 2004 shows that

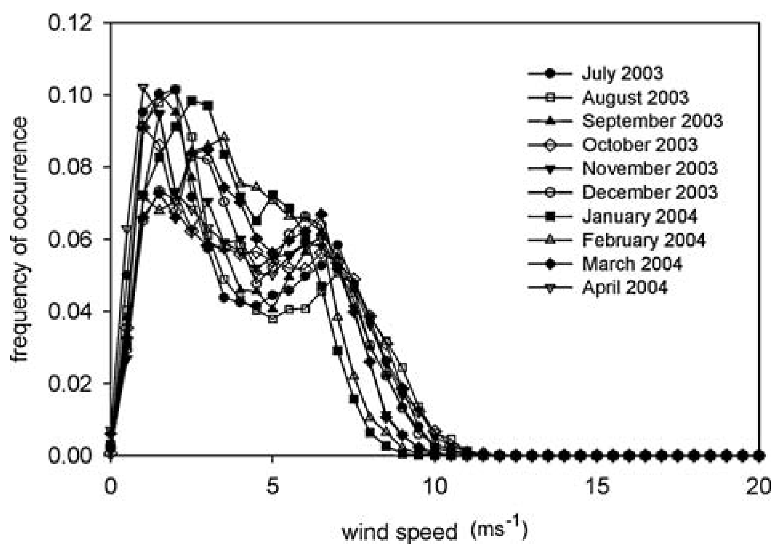

Fig 10. Frequency distribution of wind speeds in (ms^{-1}) at Rio de La Paz for the months July 2003–April 2004; bin size 0.75 × 0.2 (ms^{-1} × ms^{-1}).

the global radiation during the day is stronger in winter than in summer because of the enhanced cloudiness during summertime. There is no day throughout the year without intense upvalley flow (threshold 3 ms^{-1}), whereas there are only 24 d with intense downvalley winds.

The alongvalley wind is the first variable q_1 for the master equation (4). It is rather close to the zonal wind. Its mean value is $\bar{q}_1 = -3.2$ ms^{-1} while q_2 with $\bar{q}_2 = 0$ is the cross-valley speed. The related *SD* is 3.0 ms^{-1} (0.8 for q_2). The mean wind is always directed upvalley but there is almost no mean wind after midnight. The mean flow is, however, -6.8 ms^{-1} in the interval 12–15 h. Thus, there is vivid upvalley flow in the afternoon. The *SD* of the crossvalley component per class is fairly constant during the day, the alongvalley wind peaks after noon. The eigenvalues of the regression model are real with decay times of $\sim$20 min during the night and just 10 min during the day. The density distribution after midnight confirms the existence of downvalley flows (see also Fig. 9). There are nights, however, with upvalley flow with a northerly component. Spreads of $\sim$2 are typical at that time. The transfer vectors show a clear tendency toward downvalley accelerations (Fig. 11) in the morning interval (6–9 h). The maximum of f is located in the upvalley part of the phase plane but downvalley flows are still possible at that time. Three hours later the distribution contains almost only downvalley flows (Fig. 12). Upvalley flow occurs rarely. The spreads in Fig. 12 show relatively little variation in the interior of the domain of states. There are maxima of $\sim$4 for southerlies and also for strong northerlies at the station but diffusion is always large in this upvalley flow situation. The sharp gradients of the spread at the boundaries of the distribution are artifacts of the plotting routine. To get a better feeling for the diffusive character of the "motion" in the phase plane, the master equation (4) is integrated in time for each class starting from an initial distribution restricted to one grid box. A "cloud" of states is forming quickly which eventually comes close to the mean distribution of this class (not shown). The results depend on the choice of the initial box and on the spread of that class. The expansion may be completed in about 1 h. In other cases, the radius of the cloud is still growing after 3 h.

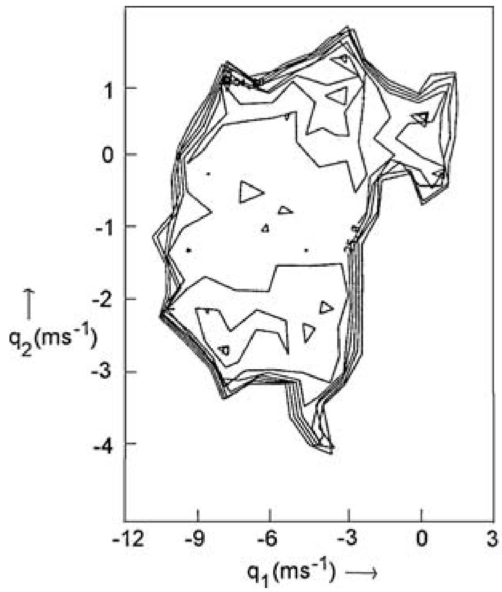

Fig 12. Spread in units of 0.1 in the interval (15–18 h). Grid points with less than 10 visits are excluded.

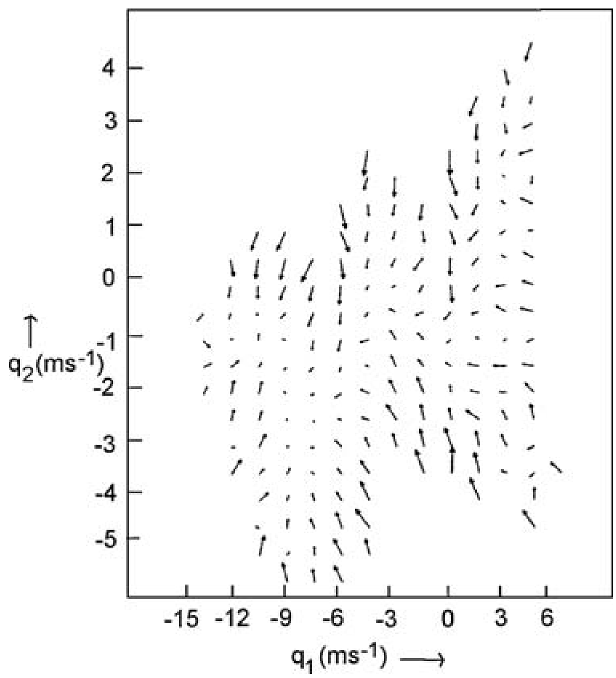

Fig 11. Transfer vector **t** in the interval (6–9 h) in the Rio de La Paz. Maximum vector length 0.9. Abscissa: along-valley wind (ms^{-1}); ordinate: cross-valley wind (ms^{-1}). Note the different scaling.

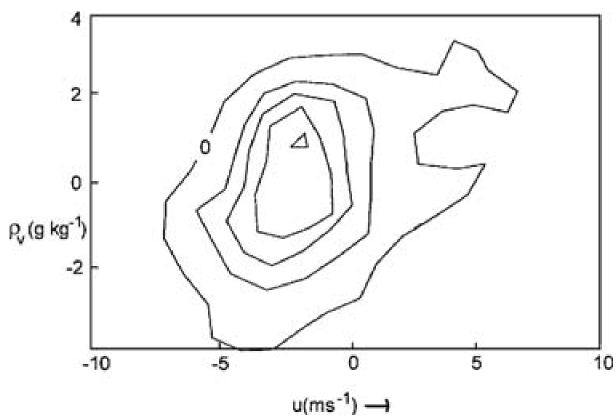

Fig 13. Density distribution in the time interval (12–15 h; $j = 6$) in units 10^{-3} at Rio de La Paz for the along-valley wind component and the water vapor density ρ_v(g kg^{-1}); bin size 0.75 × 0.5 (ms^{-1} × g kg^{-1}).

It is of particular interest to consider the data pair (q_1, ρ_v) where q_1 is the alongvalley component and ρ_v the density of water vapor. One would expect a negative correlation of both variables if the upvalley flow originates in the moist low lands. Instead, a positive correlation coefficient of 0.37 is found. The moisture content is higher during the night than the day. It is seen from Fig. 13 that the distribution in class 6 (15–18 h) has an upward tilt. Strong upvalley flows are drier than weak ones. This suggests that the air flowing up the valley descended at least partly from the higher levels.

As stated above, the model results of Zängl and Egger (2005) suggest that there is a strong upvalley flow downstream of the permanent station (see Fig. 8). To clarify this point, additional measurements have been made in May 2005 near the branching point of the valley downstream of the permanent station (see Fig. 8) at two radiation days in order to verify the model result of Zängl and Egger (2005). In contrast to the simulations, the observations revealed a late onset of the upvalley flow in the afternoon there and wind velocities less than those typically observed at the permanent station. It is likely that this discrepancy is caused by the "coarse" resolution of 2 km in the simulations of Zängl and Egger (2005). The complicated and extremely steep topography of this valley is not sufficiently resolved by the model.

5. Conclusions

It has been found that the diurnal circulation of the Altiplano leaves a clear imprint in the Tambo Quemado data. Typically, there is an easterly upslope wind after sunrise which is then slowly replaced by the westerly winds of the diurnal inflow. In the night, westerly downslope winds prevail. The model results of Zängl and Egger (2005) are in good agreement with these findings. On the other hand, there are many days where the easterly upslope wind does not evolve and westerlies dominate. It is likely that this reflects the influence of the large-scale circulation which goes mainly with westerlies in this region. All in all, the observations at Tambo Quemado establish the existence of diurnal inflow toward the Altiplano even through a pass with complicated topography on its western inflow side.

The diurnal wind system in the valley of the Rio de La Paz is extremely reliable and recurrent. The upvalley winds are found almost every day and transport air into the interior of the Altiplano. It is, however, completely open to what extent these winds contribute to the overall diurnal circulation of the Altiplano. The relative dryness of the upvalley winds suggests that the air arriving at the permanent station during the day does not originate in the humid lowlands but descends from higher levels. Thus the valley wind system of La Paz appears to be partly closed within the extent of the Altiplano.

Master equations turned out to be a useful tool for the valley wind research. They provide a much deeper and more detailed insight into the structure of the flows observed than the regression model.

6. Acknowledgment

We are grateful for the reviewer's perceptive and detailed comments which helped to improve the presentation. This work has been supported by Volkswagenstiftung.

References

Crommelin, D. 2004. Observed nondiffusive dynamics in large-scale atmospheric flow. *J. Atmos. Sci.* **61**, 2384–2396.

Egger, J. 2001. Master equations for climatic parameter sets. *Clim. Dynam.* **18**, 169–177.

Egger, J. 2002. Master equations for Himalayan valley winds. *Stochastics and Dynamics* **2**, 381–394.

Egger, J., Bajrachaya, S., Heinrich, R., Kolb, P., Lämmlein, S. and co-authors, 2002. Diurnal winds in the Himalayan Kali Gandaki valley. Part III: Remotely piloted aircraft soundings. *Mon. Weather Rev.* **130**, 2042–2058.

Egger, J., Blacutt, L. Ghezzi, F. Heinrich, R., Kolb, P. and co-authors, 2005. Diurnal circulation of the Bolivian Altiplano. Part I: Observations. *Mon. Weather. Rev.* **133**, 911–924.

Flohn, H. 1953. Hochgebirge und allgemeine Zirkulation II. Die Gebirge als Wärmequellen (in German). *Arch. Meteorol. Geophys. Biokl.* **A5**, 265–279.

Spekat, A., Heller-Schulze, B. and Lutz, M. 1983. Über Groβwetter ünd Markov-Ketten (in German). *Meteor. Rundschau* **36**, 243–248.

Torrez, R., Ghezzi, F. and Palenque, E. 2005. Algunas caracteristicas meteorologicas de la localidad de Tambo Quemado. *Rev. Fis. Bol.*, in press.

Zängl, G. and Egger, J. 2005. Diurnal circulation of the Bolivian Altiplano. Part II: Theoretical aspects. *Mon. Weather Rev.* in press.

Zwanzig, R. 2001. *Non-Equilibrium Statistical Mechanics*. Oxford, Oxford University Press 222.